Broadband Phase Resolving Spectrum Analyzer Measurement for EMI Scanning Applications

Zongyi Chen[†1], Shubhankar Marathe[*2], Hamed Kajbaf[‡3], Stephan Frei[†4], David Pommerenke[*5]

[†] TU Dortmund University, Dortmund, Germany
[1]zongyi.chen@tu-dortmund.de, [4]stephan.frei@tu-dortmund.de
[*] EMC Laboratory, Missouri University of Science and Technology. Rolla, MO, USA
[2]skmcr4@mst.edu, [5]davidjp@mst.edu
[‡] Amber Precision Instruments, San Jose, CA, USA
[3]hamed@amberpi.com

Abstract— **EMI scanning application requires phase and magnitude information for the creation of equivalent radiation models and for far-field prediction. Magnitude information can be obtained using rather an inexpensive spectrum analyzer (SA). Phase-resolving instruments such as vector network analyzers (VNA) or oscilloscopes are very expensive for frequencies above 5 GHz. For this reason, this paper proposes a method that utilizes a SA for phase-resolved magnitude measurements. The basic principle is to measure the sum or difference of two signals for different phase shifts and deduct the phase from the combined output of those measurements. The phase is retrieved using an optimization procedure. It is shown that the proposed approach can recover phase deviation within 20° when using six steps of variable attenuator control voltage for the test cases between 5 and 12 GHz.**

***Keywords*— EMI scanning, phase-resolved measurements, spectrum analyzer (SA)**

I. INTRODUCTION

In many EMC applications, phase information of measured fields is desired in addition to conventional magnitude-only measurements. Among these applications, near-field scanning benefits strongly as source reconstruction or the application of Huygens surfaces becomes possible if phase-resolved field data is provided. Other applications of phase-resolved near-field measurement are near-field to far-field transformation (NFFFT) [1-3], emission source localization methods such as emission source microscopy (ESM) [4], near-field analysis based on the surface equivalence principle (Huygens' principle) [1, 5, 6], etc.

Several practical methods are proposed in the literature to measure or calculate phase from frequency domain or time domain measurements. The method used in [2] measures the field in time domain using an oscilloscope, converts the data to frequency domain using fast Fourier transform (FFT), and finally extracts the phase information by subtracting the measurement phase from the phase of a reference probe. The drawback of this method is the cost and lab availability of oscilloscopes for higher frequencies (above 4 GHz).

On the other hand, the method used in [4] and [6] measures the field in the frequency domain using a vector network analyzer (VNA). VNA is a precise instrument for measuring magnitude and phase. However, usually the VNA measures the phase with respect to internal RF source of the instrument for S-parameter measurement. As proposed in [4], the tuned receiver mode of a VNA can be used for phase measurement with respect to an external source. The drawback of this method is poor image and spurious rejection of many VNAs in tuned receiver mode which leads to difficulties if the spectrum contains many signals, including pulsed and broadband signals other than the signal of interest.

Availability and low cost of spectrum analyzers (SA) at very high frequencies makes them suitable for near field scanning. Another advantage is offered by different types of detectors, such as quasi-peak or average detectors which are required for EMI measurements. However, SAs are only able to resolve magnitude or I/Q components relative to its own signal source, which makes it unsuitable for EMI scanning if both phase and magnitude of field data are desired. This paper proposes a practical, broadband swept frequency method for magnitude and phase measurement using SA.

Usually, in phase-resolved scanning, one probe (field probe) is moved and a phase reference signal is taken from a fixed location, either via a second probe (reference probe) or by directly accessing a signal within the device under test (DUT) [1, 4]. In [8-9], a method is described that determines the phase from multiple SA measurements. In this method, a 0° hybrid coupler sums the field probe and the reference probe signals. To retrieve the phase, at least three sweeps are required. Each sweep uses a different configuration for the sum of the signals. However, the method fails to obtain useful phase information if the magnitude difference between the reference probe and the field probe signals is large. This is a result of using the magnitude change of vector additions at different phase angles. If the phase of the smaller signal is changed, the magnitude of the sum will change very little. Furthermore, the method in [8] has been described for only single frequency application.

This paper discusses how to overcome both limitations, since the SA method allows phase measurements of many frequencies to be taken simultaneously and is less sensitive to differences in magnitude between the field probe and the reference probe signals. Similar to [8-9], the proposed method uses combinations of the field probe and the reference probe signals. However, the measurement is performed at different reference probe signal attenuation levels. In this way, it is ensured that for one measurement data set the field probe and the reference probe have similar magnitudes. This allows the phase to be resolved even if the field probe and reference probe signal amplitudes are very different. The SA method was tested using a comb generator to create signals from 5 to 12 GHz every 200 MHz and a voltage variable attenuator with a 30 dB adjustment range.

II. PRINCIPLES

Similar to [8-9], the field probe and the reference probe signals are combined using different phase shifts. The combination can be achieved by taking the sum and/or the difference. The analysis of the methods presented in [4-5] showed that the SA method only works if the magnitudes of the field probe and reference probe signals are similar. To overcome this, a variable attenuator was added. If the combinations of the field probe and reference probe signals are measured multiple times (for example, at six different settings of voltage-controlled attenuator). There will be an attenuator setting at which the magnitudes of the field probe and the reference probe are similar, provided that the field probe signal is very weak. If its magnitude is too weak then it's also not significant for many EMI applications. For the verification of the concept, arbitrary signals are used instead of probes. However, using signals from probes with sufficient low noise amplification is a straightforward change to the system, thus, only the phase resolving has been investigated for this paper.

Two setups have been implemented in this research:

I. Using the sum and difference for two different cable lengths in the reference branch, producing two different phase shifts (shown in Fig. 1).
II. Using only the sum for three different cable lengths in the reference branch, producing three different phase shifts (shown in Fig. 2).

Setup-II was developed to avoid the expensive broadband 180° hybrid coupler shown in setup-I.

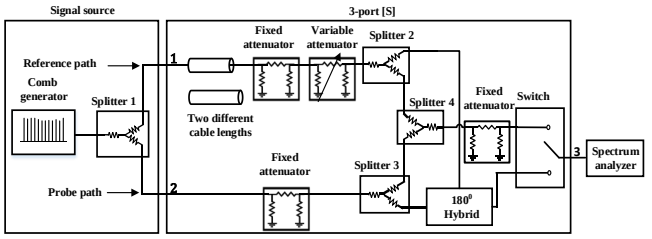

Fig. 1 Block diagram of setup-I

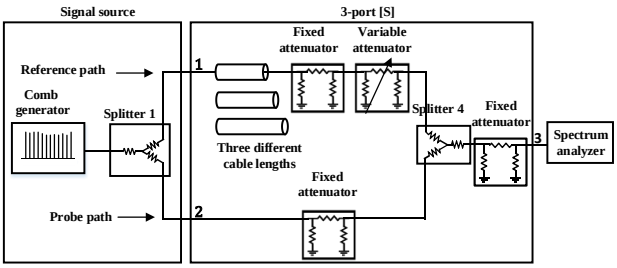

Fig. 2 Block diagram of setup-II

In this experiment, six attenuation levels adjusted by voltage-controlled variable attenuator have been used for both setups, and each setup is characterized by its 3-port S-parameters. The setups are as follows:

- Setup-I: six attenuator settings and two cables resulting in 12 S-parameter sets.
- Setup-II: six attenuator settings and three cables resulting in 18 S-parameter sets.

Fixed attenuators are used to improve the input match such that input reflections can be neglected. In a real scanning setup, amplifiers would be in the field probe and reference probe paths, so additional loss of the attenuators would not diminish the system noise figure, and possible reflections between the amplifiers and the system would be expressed in the S-parameter set.

Setup-II simply replaced the expensive 180° hybrid coupler. Therefore, only the mathematical calculation is demonstrated for setup-I. At each attenuator setting four sweeps were performed. Measured sum and difference of power were recorded for the shorter phase shift cable as $P_{meas\Sigma}$ and $P_{meas\Delta}$, respectively. Using a longer cable length (=phase shift), two more sweeps were carried out and the results are denoted by $P_{meas\Sigma\_s}$ and $P_{meas\Delta\_s}$.

Expressing the output signals by the S-parameters of the system leads to:

$$\begin{aligned}\left|b_{3\_meas\Sigma}\right|^2 &= \left|S_{31\Sigma}a_1+S_{32\Sigma}a_2\right|^2 \\ &= |S_{31\Sigma}|^2|a_1|^2 + |S_{32\Sigma}|^2|a_2|^2 \\ &\quad + 2|S_{31\Sigma}||a_1||S_{32\Sigma}||a_2|\,cos(\emptyset_{1\Sigma} \\ &\quad - \emptyset_{3\Sigma} + \varphi)\end{aligned} \tag{1}$$

$$\begin{aligned}\left|b_{3\_meas\Delta}\right|^2 &= \left|S_{31\Delta}a_1+S_{32\Delta}a_2\right|^2 \\ &= |S_{31\Delta}|^2|a_1|^2 + |S_{32\Delta}|^2|a_2|^2 \\ &\quad + 2|S_{31\Delta}||a_1||S_{32\Delta}||a_2|\,cos(\emptyset_{1\Delta} \\ &\quad - \emptyset_{3\Delta} + \varphi)\end{aligned} \tag{2}$$

$$\begin{aligned}\left|b_{3\_meas\Sigma\_s}\right|^2 &= \left|S_{31\Sigma\_s}a_1+S_{32\Sigma\_s}a_2\right|^2 \\ &= \left|S_{31\Sigma_s}\right|^2|a_1|^2\left|S_{32\Sigma_s}\right|^2|a_2|^2 + \\ &\quad 2\left|S_{31\Sigma\_s}\right||a_1|\left|S_{32\Sigma\_s}\right||a_2|\,cos\left(\emptyset_{1\Sigma\_s}\right. \\ &\quad \left. - \emptyset_{3\Sigma\_s} + \varphi\right)\end{aligned} \tag{3}$$

$$\begin{aligned}\left|b_{3\_meas\Delta\_s}\right|^2 &= \left|S_{31\Delta\_s}a_1+S_{32\Delta\_s}a_2\right|^2 \\ &= \left|S_{31\Delta\_s}\right|^2|a_1|^2 + \left|S_{32\Delta\_s}\right|^2|a_2|^2 + \\ &\quad 2\left|S_{31\Delta\_s}\right||a_1|\left|S_{32\Delta\_s}\right||a_2|\,cos\left(\emptyset_{1\Delta\_s} -\right. \\ &\quad \left.\emptyset_{3\Delta\_s} + \varphi\right)\end{aligned} \tag{4}$$

where $S_{31\Sigma}$, $S_{32\Sigma}$ are S-parameters measured if the system is configured to measure the sum $P_{meas\Sigma}$ using the shorter cable,

$S_{31\Sigma\_s}$, $S_{32\Sigma\_s}$ are S-parameters measured if the system is configured to measure the sum $P_{meas\Sigma\_s}$ using the longer cable,

$S_{31\Delta}$, $S_{32\Delta}$ are S-parameters measured if the system is configured to measure the sum $P_{meas\Delta}$ using the shorter cable,

$S_{31\Delta\_s}$, $S_{32\Delta\_s}$ are S-parameters measured if the system is configured to measure the sum $P_{meas\Delta\_s}$ using the longer cable,

$\emptyset_{1\Sigma}$ is the phase of $S_{31\Sigma}$, $\emptyset_{3\Sigma}$ is the phase of $S_{32\Sigma}$,
$\emptyset_{1\Delta}$ is the phase of $S_{31\Delta}$, $\emptyset_{3\Delta}$ is the phase of $S_{32\Delta}$,
$\emptyset_{1\Sigma\_s}$ is the phase of $S_{31\Sigma\_s}$, $\emptyset_{3\Sigma\_s}$ is the phase of $S_{32\Sigma\_s}$,
$\emptyset_{1\Delta\_s}$ is the phase of $S_{31\Delta\_s}$, $\emptyset_{3\Delta\_s}$ is the phase of $S_{32\Delta\_s}$,
φ is phase difference, $\varphi = \emptyset_{a2} - \emptyset_{a1}$.

The input parameters for equations (1) through (4) are $|a_1|$, $|a_2|$ and φ. Here, $|a_1|$ is the reference probe signal from a fixed location. It can be measured once before the scan. Thus, $|a_1|$ is known. The unknowns are $|a_2|$ and φ.

For solving these unknown parameters, an optimization algorithm is applied to $|a_2|$ and $\emptyset_{a2}, \emptyset_{a1}$. The optimization iteratively minimizes the error between calculated SA power and measured SA value. This requires a set of starting values for $|a_2|$ and $\emptyset_{a2}, \emptyset_{a1}$, then the calculated power can be obtained using:

$$P_{calcu\Sigma} = \frac{1}{2}\left|b_{3\_start\Sigma}\right|^2 = \frac{1}{2}\left|S_{31\Sigma}a_{1\_start} + S_{32\Sigma}a_{2\_start}\right|^2 \quad (5)$$

$$P_{calcu\Delta} = \frac{1}{2}\left|b_{3start\Delta}\right|^2 = \frac{1}{2}\left|S_{31\Delta}a_{1\_start} + S_{32\Delta}a_{2\_start}\right|^2 \quad (6)$$

$$P_{calcu\Sigma\_s} = \frac{1}{2}\left|b_{3start\Sigma\_s}\right|^2 = \frac{1}{2}\left|S_{31\Sigma\_s}a_{1\_start} + S_{32\Sigma\_s}a_{2\_start}\right|^2 \quad (7)$$

$$P_{calcu\Delta\_s} = \frac{1}{2}\left|b_{3start\Delta\_s}\right|^2 = \frac{1}{2}\left|S_{31\Delta\_s}a_{1\_start} + S_{32\Delta\_s}a_{2\_start}\right|^2 \quad (8)$$

where $a_{1\_start} = |a_1|e^{j\emptyset_{a1\_start}}$

$a_{2\_start} = |a_{2\_start}|e^{j\emptyset_{a2\_start}}$

Similar to other optimization functions, the convergence and accuracy of the combined results highly depend on the definition of the error function value which is minimized. Here, the error function is defined in dB by:

$$Error_{total} = Error_{\Sigma} + Error_{\Delta} + Error_{\Sigma\_s} + Error_{\Delta\_s} \quad (9)$$

where $Error_{\Sigma} = |P_{meas\Sigma} - P_{calcu\Sigma}|$,
$Error_{\Delta} = |P_{meas\Delta} - P_{calcu\Delta}|$,
$Error_{\Sigma\_s} = |P_{meas_{\Sigma\_s}} - P_{calcu_{\Sigma\_s}}|$, and
$Error_{\Delta\_s} = |P_{meas\Delta\_s} - P_{calcu\Delta\_s}|$.

A potential problem lies in reaching the local minima. This can be avoided by optimizing the starting values, which may require testing different starting values and accepting the converged result (showing the lowest error value) as the best estimate of the global minima. In its present un-optimized Matlab implementation, the optimization takes several seconds.

III. Implementation

Block diagram and actual picture of Setup-I have been shown in Fig. 1 and Fig. 3, respectively. The test signal was created using a comb generator and splitter 1, also shown in Fig. 1. A fixed attenuator of 6 dB was applied in the reference probe path and 20 dB in the field probe path. A 5 dB fixed attenuator was applied to the output of splitter 4. The fixed attenuators were introduced to mitigate multiple reflections and to observe how the proposed method performs while having power level differences between the field probe and the reference probe signals.

The different attenuators in the field probe and reference probe paths led to a 14 dB difference in the signal strength within the phase resolving system. Thus, the effect of the fixed attenuator was compensated by a 14 dB setting of the variable attenuator, as shown in Fig. 4 with a black line representing an attenuator control voltage equal to -1.5 V. It was expected that the lowest phase error was achieved at this setting. The measured 3-port system S-parameters are shown in Fig. 5. In this figure, S_{31} represents the reference probe path and S_{32} represents the field probe path. The black box emphasizes the region where the magnitude of S_{31} is similar to S_{32}, which verifies the proper behavior of the variable attenuation settings.

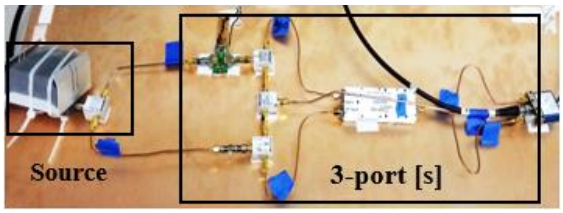

Fig. 3 Measurement setting for setup-I

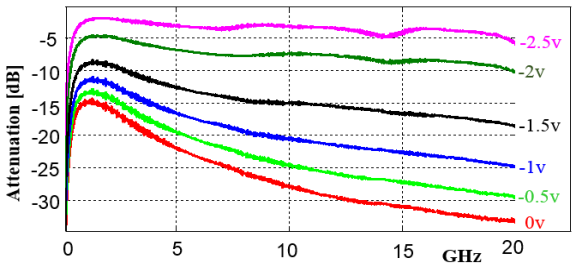

Fig. 4 Voltage-controlled variable attenuator

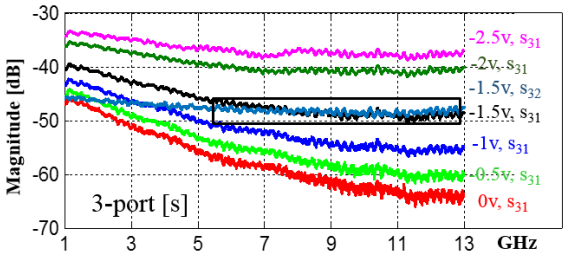

Fig. 5 System S-parameter corresponds to variable attenuator control voltages (setup-I)

Setup-II, shown in Fig. 6, avoids the use of expensive 180° hybrid coupler, which is identical to a 0° splitter and an inverter. One option is to build an inverter and use a splitter, and another is to introduce a third phase shift using cables. For a broadband method it is not possible to choose one cable length which gives a phase shift of 180° for all frequencies. As shown in Fig. 7, using three cables provides enough phase shift at every investigated frequency. For example, taking a frequency of 8 GHz, the phase difference between the reference probe signal ("ref" in red) and cable I ("phase I" in green) is 25°, and the phase difference between the reference probe signal ("ref" in read) and cable II ("phase II" in blue) is 85°. For setup-II, fixed attenuators of 16 dB and 10 dB are applied to the field probe

path and the reference probe path respectively. This results in a different optimal variable attenuator setting—as shown in Fig. 4. An attenuator control voltage of -2 V leads to additional 6 dB attenuation in reference probe path

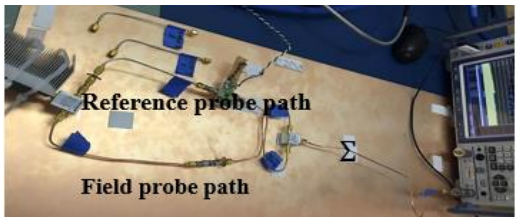

Fig. 6 Measurement setting for setup-II

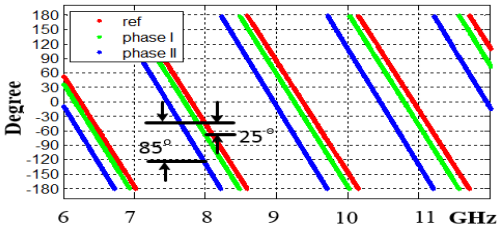

Fig. 7 Three phase shift cables–phase information

Multiple reflections between the system output (port 3, Fig. 2) and the SA will impact the phase and magnitude retrieval accuracy. Every SA has a non-zero reflection coefficient. In this paper, a voltage standing wave ratio of (VSWR) = 1.8 (worst case Rohde & Schwarz model FSV for 3.6 to 20 GHz) is used for calculating level error ΔL_r (shown in Fig. 8) in dB due to mismatch using:

$$\Delta L_r = 20 \cdot \log(1 - r_s \cdot r_l) \qquad (10)$$

where r_s represents the magnitude of the reflection coefficient of the system's output port (port 3, Fig. 2), which equals S_{33} of the system S-parameters and r_l is the magnitude of SA's reflection coefficient.

Adding a 5 dB attenuator reduces the impact of multiple reflections. Using an input attenuator setting larger than 0 dB or a 10 dB attenuator will further reduce the effect of multiple reflections. This will not impact the system's sensitivity providing that the field probe signals are sufficiently amplified using a low noise amplifier as the first stage amplifier.

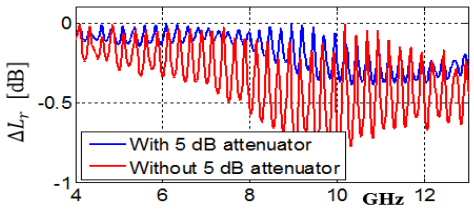

Fig. 8 Calculated level error with/without added attenuator as a result of mismatch for setup-II

IV. Measurement Results

To validate the method, a broadband signal was created using an Omniyig comb generator. The source spectrum measured after splitter 1 is shown in Fig. 9. The splitters are rated up to 12 GHz; for this reason the analysis was performed for the signals between 5 and 12 GHz.

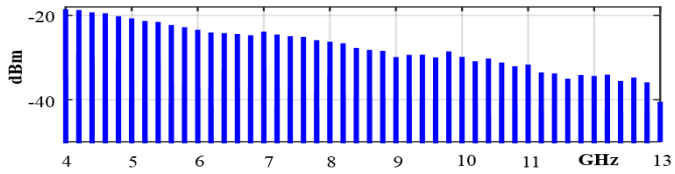

Fig. 9 Source power spectrum after splitter 1

Reference probe signal and field probe signal were obtained from the output signal of in-phase splitter 1, which means that $|a_1|$ and $|a_2|$ are known and $\varphi = 0°$. A known phase shift cable was then introduced to the reference probe path to create an out-of-phase reference probe signal and field probe signal. This allows comparison of the calculated phase and magnitudes to the real values of $|a_1|, |a_2|$ andφ. In this paper, power "measured" means power directly measured by the SA. Power "calculated" means power calculated using the measured S-parameters and the measured splitter 1 output values. Power "retrieved" means power retrieved using measured power at the SA as input for the optimization.

A. Measurement results for setup-I

Due to the large amount of cables, splitters, and the usage of a voltage-controlled attenuator the system's S-parameters are prone to error. We have observed variations from repeated dismounting, mounting, and S-parameter measurements in the range of +/- 0.5 dB. To test the effect of such errors and inaccuracies of the SA readings or time variations of the DUT emissions, simulations were performed that use the correct field probe and reference probe input signals and phases to calculate the power value that the SA would measure if the S-parameters were perfect. These calculated powers were then compared to the power measured by the SA.

As a representative example of the observed overall behavior, the data is shown in Fig. 10 for 8 GHz. Here, the dashed line with diamond marker denotes the power directly measured by the SA and the solid line with star marker denotes the power calculated using the measured S-parameters and the measured splitter 1 output values. The data match within ±0.5 dB. The black circle indicates a case in which the phase shifts add up in such a way that the sum turns into a difference, which led to a minimum in the SA reading when the attenuator control voltage was -1.5 V. Such a cancellation point is rather sensitive to small phase and magnitude errors. The fact that a good match is achieved at such a cancellation point is an indicator for the robustness of the method.

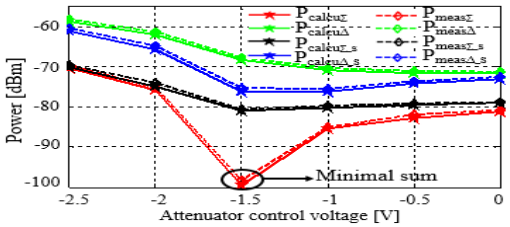

Fig. 10 Power measured compared with power calculated for setup-I

In real scan, the reference probe (from which the reference signal can be obtained) was at a fixed location. Thus, the reference signal magnitude spectrum could be measured once before the scan. The reference signal magnitude spectrum was known. The optimization algorithm only needed to retrieve the field probe power, and phase difference between the reference probe and field probe signals. The correct phase difference between the reference probe and field probe signals of the test setup was 0°. As an in-phase splitter was used to create the field probe and reference probe signals (shown in Fig. 1, splitter 1), the retrieved field probe power should have been the same as the reference probe power. The results are shown in Fig. 11 at 9 GHz and 11 GHz. For both frequencies, the retrieved field probe power shows a good agreement to the reference probe power among all attenuator settings. However, the retrieved phase shows more sensitivity to the attenuator setting. It was expected that the best phase recovery would be obtained at the attenuator setting, which leads to similar reference probe and field probe magnitudes at the splitter (shown in Fig. 1, splitter 4). Figure 11 indicates the same behavior as expected. At an attenuator control voltage of -1.5 V (the condition in which the variable attenuator produces a 14 dB attenuation to get similar reference probe and field probe signal levels), a phase error in the range of 10° was observed. This was most likely due to a sensitivity to an incorrect SA power measurement.

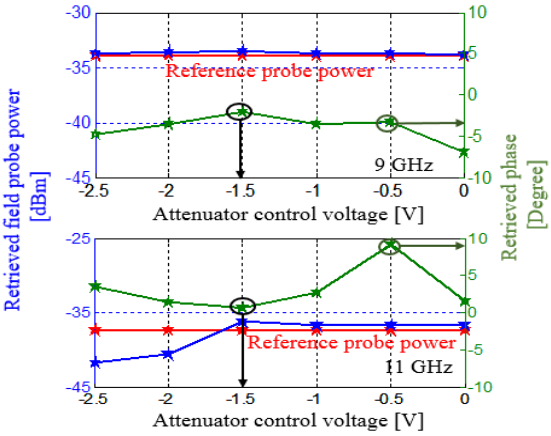

Fig. 11 Retrieved phase, field probe power (setup-I)

The power measured by the SA is not an exact value. Errors can be introduced by time variation of the EMI signals of a DUT and by inaccuracies of the SA itself. To investigate the robustness of the phase and field probe power retrieval, the following numerical experiments have been conducted. Using the correct SA readings (four power measures for each variable attenuator setting, $P_{meas\Sigma}$, $P_{meas\Delta}$, $P_{meas\Sigma\_s}$, and $P_{meas\Delta\_s}$), a random distributed variation uniformly distributed at ±2.5 dB was added to the correct values. The distributed values were then added to the optimization process to identify the best fitting field probe powers and phase values. This was repeated 1000 times for different combinations of the distributed values. Each of the 1000 trials resulted in one best estimate of the field probe power and one estimate of the phase. Those results are illustrated in Fig. 12 for 7 GHz as histograms.

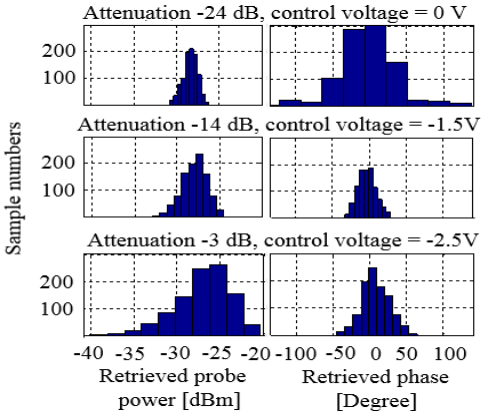

Fig. 12 Histogram of the retrieved field probe power (left) and the retrieved phase (right)

B. *Measurement results for setup-II*

The setup-II used three different cable lengths for the phase shift instead of the hybrid coupler. First, an in-phase reference probe and field probe signal case was tested. Only the test set-up changed; the power capture and post-processing was similar to that of setup-I. The retrieved field probe powers and retrieved phases at 7 GHz are shown in Fig. 13. The retrieved field probe powers followed the reference probe powers and a less than 1 dB deviation was observed. The retrieved phases were less than 20° when attenuator control voltage varied from -2.5 V to -1.5 V (best range).

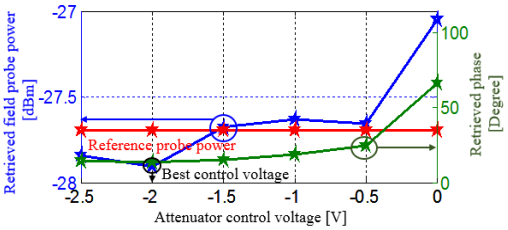

Fig. 13 Retrieved results for in-phase reference probe and field probe signals (setup-II)

Furthermore, an out-of-phase reference probe and field probe signal case was also verified. An additional phase shift was introduced to the reference channel so that a phase difference could be detected between the reference probe and the field probe signals. The results of the configuration are shown in Fig. 14. The retrieved field probe power has less than 1 dB error for all attenuation settings. The phase was best retrieved at an attenuator setting of -2 V (= 7.5 dB attenuation). At that voltage, the field probe signal and the attenuated reference probe signal have about the same magnitude at splitter 4. Thus, the effect of adding different phase angles led to the largest magnitude changes. For an attenuator setting of 0 V (= 24 dB attenuation), the magnitude difference is too large such that the phase retrieval fails.

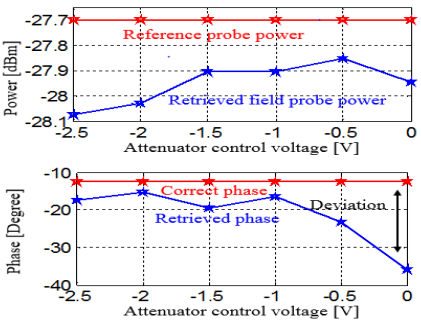

Fig. 14 Retrieved results for out-of-phase reference probe and field probe signal (setup-II)

V. Discussion

In this paper, the phase information of a broadband signal is recovered within ±20° of the actual phase value. As discussed in [6] and [10], far-field calculations based on the Huygens' box are rather insensitive to phase errors if the maximal signal is of interest. Since the magnitude errors are in the range of 1 dB, the proposed method could be practically used for this type of application

The analysis presented here shows two setups for phase measurement. By controlling the reference signal level a good phase measurement accuracy could be reached. However, a set of limitations needs to be considered. Using different switchable attenuators, the frequency range of the hardware can be increased from a few MHz to 20 GHz, but the accuracy would suffer from the required phase shifts. If only one extra length cable and a 180° hybrid coupler is used as shown in Fig. 2, the selection of the cable length would be required on one side to have a reasonable phase change at the lowest frequency, but not to reach 360° at the highest frequency. If it would shift the phase by 360°, no net effect would be achieved. If the lowest phase shift is estimated to be 30° and the largest is estimated to be 300° then a 1:10 frequency range may be achievable.

The comb generator covered a range from -39 to -27 dBm between 5 and 12 GHz. The spectral components of the signals of interest usually also cover a limited amplitude range, as the lowest signals are generally of no interest from an EMI point of view. The range of the amplitudes that can be phase resolved depends on the attenuations used in the reference channel. A stepping of about 5 dB revealed good data. Much larger steps would reduce accuracy. Thus, to cover a range of 30 dB, six steps are needed resulting in 18 sweeps at each scan point (setup-II) and 24 sweeps (setup-I). We assume that the number of sweeps could be further reduced, but it will require more experience with the SA method. In summary, broadband phase-resolved scanning using an SA is possible, however, additional hardware is needed and the scan time increases.

VI. Conclusion

EMI scanning often requires phase- and magnitude-resolved field data. A broadband method to capture phase and magnitude data using an SA is discussed. Using a variable attenuator to match power levels of the reference probe and field probe signals can increase the phase measurement accuracy significantly. The presented implementation requires minimum 18 sweeps at each test point. Using 100 kHz resolution bandwidth and a sweep from 6 to 9 GHz and 30000 points a sweep time of 30 ms was measured on an FSV-30 (Rohde & Schwarz) SA. Assuming 20 ms for data transfer this leads to a scan time per point of about 2 seconds including 1 sec to move the probe. For lower RBW a list sweep (only measure frequencies of interest) is advisable to keep the sweep time acceptably low. In its present un-optimized Matlab implementation the optimization requires several seconds. With the investigated configurations phase was recovered within an error margin of about ±20°.

Acknowledgment

This material is based upon work supported partially by the National Science Foundation under Grant No. IIP-1440110 and the work is supported in part by the scholarship from China Scholarship Council (CSC).

References

[1] K. Kam, A. Radchenko, and D. Pommerenke, "On different methods to combine cable information into near-field data for far-field estimation," *in Proc. IEEE Int. Symp. Electromagn. Compat.*, pp. 294-300, August 2012.

[2] J. Zhang, K. W. Kam, J. Min, V.V. Khilkevich, D. Pommerenke, and J. Fan, "An effective method of probe calibration in phase resolved Near-field scanning for EMI application," *IEEE Trans. Instrum. Meas.*, vol. 62, no. 3, pp. 648-658, March 2013.

[3] J. Zhang., Source reconstructions for IC radiated emissions based on magnitude-only near-field scanning, Ph.D. dissertation, EMC lab, Missouri S&T., Rolla, MO, USA, 2013.

[4] P. Maheshwari,V. Khilkevich, D. Pommerenke, H. Kajbaf, and J. Min, "Application of emission source microscopy technique to EMI source localization above 5 GHz," *IEEE Int. Symp. Electromagn. Compat.*, pp. 7-11, August 2014.

[5] X. Gao, J. Fan, Y. Zhang, H, Kajbaf, and D. Pommerenke, "Far-field prediction using only magnetic near-field scanning for EMI test," *IEEE Trans. Electromagn. Compat.*, vol. 56, no. 6, pp. 1335-1343, December 2014.

[6] M. Sorensen, O. Franek, G. Pedersen, A. Radchenko, K. Kam, and D. Pommerenke, "Estimate on the uncertainty of predicting radiated emission from Near-field scan caused by insufficient or inaccurate Near-field data," *IEEE Int. Symp. Electromagn. Compat.*, pp. 1-6, September 2012.

[7] A. Ramanujan, H. Shall, Z. Riah, F. Lafon, and M. Kadi, "From complex near-field measurements to radiated emissions modelling of electronic equipments," *IEEE Int. Symp. Electromagn. Compat.*, pp. 97-101, September 2014

[8] Y. Vives , C. Arcambal , A. Louis , F. de Daran, P. Eudeline, and B. Mazari, "Modeling magnetic radiations of electronic circuits using near-field scanning method," *IEEE Trans. Electromagn. Compat.*, vol. 49, no. 2, pp. 391-400, May 2007.

[9] Gilabert, Y. V. Modélisation des émissions rayonnées de composants électroniques. Ph.D. dissertation, Université de Rouen, 2007.

[10] A. Radchenko, J. Zhang, K. Kam, and D. Pommerenke, "Numerical evaluation of near-field to far-field transformation robustness for EMC," *IEEE Int. Symp. Electromagn. Compat.*, pp. 605-611, August 2012